Data-Based Fault-Tolerant Control of High-Speed Trains with Traction/Braking Notch Nonlinearities and Actuator Failures

Qi Song and Yong-Duan Song

Abstract—**This paper investigates the position and velocity tracking control problem of high-speed trains with multiple vehicles connected through couplers. A dynamic model reflecting nonlinear and elastic impacts between adjacent vehicles as well as traction/braking nonlinearities and actuation faults is derived. Neuroadaptive fault-tolerant control algorithms are developed to account for various factors such as input nonlinearities, actuator failures, and uncertain impacts of in-train forces in the system simultaneously. The resultant control scheme is essentially independent of system model and is primarily data-driven because with the appropriate input–output data, the proposed control algorithms are capable of automatically generating the intermediate control parameters, neuro-weights, and the compensation signals, literally producing the traction/braking force based upon input and response data only– the whole process does not require precise information on system model or system parameter, nor human intervention. The effectiveness of the proposed approach is also confirmed through numerical simulations.**

Index Terms—**Data-based, fault-tolerant, input nonlinearities, neuroadaptive control.**

I. Introduction

CONTROL technology plays an important role in maintaining safe, reliable, and cost-effective operation of trains. Various control techniques for automatic train operation have been reported in the literature [1]–[11]. It is noted that most existing methods are based on the single point-mass model, and the coupling elastic dynamics among the vehicles are ignored. However, in comparison with the single point-mass model, the multiple point-mass model is more practical, and several researchers have tackled various control issues of cargo and passenger trains based on multiple point-mass model coupled with in-train forces in the past few years [12]–[17]. Note that in practice it is difficult to model or measure the impacts of in-train forces. Furthermore, the basic resistive forces become increasingly significant as the train speed increases. In addition, as the traction/braking notches are used in train operation, input nonlinearities are involved in the underlying dynamics.

To enhance the control performance of uncertain nonlinear vehicle systems, different control methods were developed and integrated utilizing respective advantages in the control system design. Proportion-integral-derivative (PID)-based (or its extend version) controllers are widely used [1]. Besides, some model-based control algorithms were developed, and fuzzy control was also proposed these years [18]. Universal function approximations such as neural networks (NNs) have been widely used in the robust control of uncertain nonlinear systems, owing to its learning and adaptive abilities. NNs together with the corresponding algorithms have been used in a wide range of application areas [19]–[29]. However, the system model or system parameters are required as *a priori* in some of the proposed methods or linearization approximation is normally exercised in control design and stability analysis.

As accurate system model as well as system parameters are difficult to obtain, new control designs for high-speed trains that are independent of system models and parameters are highly desirable. In this paper, our particular interest lies in control design that demands little information on system model and parameters–we attempt to build control schemes upon input–output data.

Considerable efforts on deriving control algorithms directly from data have been made during the past decades [30]–[35], where various names or terminologies have been used, that is, data-based, data-driven, unfalsified, model-free, and model-independent control. In some sense, data-based control can be viewed as the direct construction of the controller from related input–output data. Perhaps the first data-driven control method is the Ziegler–Nichols procedure for tuning PID controllers, which is based on the plant step response. In the literature, neuro-fuzzy is also considered as data-driven control, which has been successfully applied to control water level as reported in [34]. Moreover, there are some other works that exclusively address the design of data-driven control for a class of systems [35]. To our best knowledge, however, little effort has been made in synthesizing a systematic data-based NN control scheme for high-speed train with consideration of traction/braking nonlinearities and possible faults in the literature.

Manuscript received January 14, 2011; revised October 24, 2011; accepted October 26, 2011. Date of publication December 9, 2011; date of current version December 13, 2011. This work was supported in part by the National Natural Science Foundation of China under Grant 60974052 and Grant 61134001, in part by the Program for Changjiang Scholars and Innovative Research Team in University under Grant IRT0949, in part by the Beijing Jiaotong University Research Program under Project RCS2008ZT002, Grant 2009JBZ001, and Grant 2009RC008, in part by the Innovation Foundation of Beijing Jiaotong University under Grant 2011YJS009, and in part by Major State Basic Research Development Program 973 (2012CB215202).

The authors are with the State Key Laboratory of Rail Traffic Control and Safety, Beijng Jiaotong University, Beijing 100044, China (e-mail: 09111018@bjtu.edu.cn; ydsong@bjtu.edu.cn).

Color versions of one or more of the figures in this paper are available online at http://ieeexplore.ieee.org.

Digital Object Identifier 10.1109/TNN.2011.2175451

This paper is concerned with movement control for banking vehicles, such as railway vehicles, and especially but not exclusively for such vehicles intended for use in high-speed railway passenger vehicles. The factors of input nonlinearities, actuator failures, and in-train forces are explicitly addressed in control design and stability analysis. A multiple point-mass model considering traction/braking notches is derived. As the impacts of in-train forces are difficult to model directly, and actuation failures might occur during system operation, robust adaptive control driven primarily by input-response data is investigated with emphasis on fault tolerance. The resultant control algorithms are independent of system model, which are derived without linearizing or approximating the nonlinear nature of resistive aerodynamic drag forces, in-train forces, and other unknown nonlinear impacts. The proposed control is primarily data-driven because with the appropriate input and response data, the proposed control algorithms are capable of automatically generating the intermediate control parameters and neuro-weights as well as the compensation signals, and eventually producing the traction/braking force F without the need for precise system model or system parameter, nor human intervention.

The remainder of this paper is organized as follows. Section II presents the multiple point-mass model considering traction/braking notches. In Section III, three neuroadaptive control schemes including the fault-tolerant control are developed. Position and velocity tracking stability are established via a formative mathematical analysis. Numerical simulation studies on a train similar to *CRH5* under various operating conditions are conducted and the results are presented in Section IV. This paper concludes with Section V.

II. Modeling and Problem Statement

This section examines the dynamic model of train consisting of multiple vehicles connected through elastic couplers, where traction/braking notches are explicitly addressed.

A. Multiple Point-Mass Model Considering Traction and Braking Notches

Following [36], consider a train consisting of n vehicles (q locomotives and p carriages) connected by n–1 nonlinear and elastic couplers and draft gears, as illustrated in Fig. 1, where x_i denotes the distance between the center of the ith vehicle and the reference point, $\Delta x_i = \vartheta_i + \Delta x_{di}$ is the length of the connector between the ith vehicle and the $(i+1)$ th one, where ϑ_i is a constant corresponding to the original length of the connector without any elastic deformation, and Δx_{di} represents the absolute extension or compression length of the ith spring connector, which could be positive or negative and is determined by [36]

$$\Delta x_{di} = x_{i+1} - x_i - d_{i+1} - d_i - \vartheta_i \tag{1}$$

where d_{i+1}, d_i, and ϑ_i are some constants. Therefore, it follows that

$$\Delta \dot{x}_{di} = \dot{x}_{i+1} - \dot{x}_i. \tag{2}$$

Note that for safe and energy-efficient operation, different notches (scales) of traction/braking forces are required during different operating phases of the train, thus actuation saturation due to traction and braking notches is involved in the train system, which motivates the consideration of the following multiple point-mass model incorporated with nonlinear traction/braking notches and nonsymmetric saturation

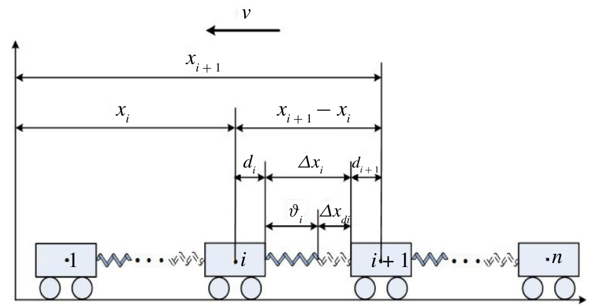

Fig. 1. Vehicles with elastic connections.

$$\begin{bmatrix} m_1 & & & \\ & m_2 & & \\ & & \ddots & \\ & & & m_n \end{bmatrix} \begin{bmatrix} \ddot{x}_1 \\ \ddot{x}_2 \\ \vdots \\ \ddot{x}_n \end{bmatrix} = \begin{bmatrix} \lambda_1 & & & \\ & \lambda_2 & & \\ & & \ddots & \\ & & & \lambda_n \end{bmatrix} \begin{bmatrix} \Psi_1(F_1) \\ \Psi_2(F_2) \\ \vdots \\ \Psi_n(F_n) \end{bmatrix} + \begin{bmatrix} 0 \\ g_1(x_2, x_1, \dot{x}_2, \dot{x}_1, p_1) \\ \vdots \\ g_{n-1}(x_n, x_{n-1}, \dot{x}_n, \dot{x}_{n-1}, p_{n-1}) \end{bmatrix} - \begin{bmatrix} g_1(x_2, x_1, \dot{x}_2, \dot{x}_1, p_1) \\ \vdots \\ g_{n-1}(x_n, x_{n-1}, \dot{x}_n, \dot{x}_{n-1}, p_{n-1}) \\ 0 \end{bmatrix} - \begin{bmatrix} f_{d1} \\ f_{d2} \\ \vdots \\ f_{dn} \end{bmatrix} \tag{3}$$

where the in-train force g_i (.) is of the form

$$g_i\,(\Delta \dot{x}_{di},\ \Delta x_{di}) = g_i\,(\dot{x}_{i+1}, \dot{x}_i, x_{i+1}, x_i, p_i) \tag{4}$$

which is essentially a nonlinear and uncertain function of $\dot{x}_i$, x_i, $\dot{x}_{i+1}$, and x_{i+1}, as well as the parameter vector $p_{i.}$ ($g_0 = 0$ and $g_n = 0$ because there is no in-train force at the front of the first vehicle and at the end of the last vehicle.) The definitions of the other variable are: m_i is the mass of the ith vehicle, which might not be accurately available due to uncertain variation of passengers and loads (the number of passengers on board each vehicle is different and uncertain in general); x_i is defined as before; $\lambda_i > 0$ is a distribution constant determining the power/braking effort of the ith vehicle; f_{di} denotes the resistive force acting on the ith vehicle. Note that the resistive force f_{di} for each vehicle takes the form

$$f_{di} = a_{0i} + a_{1i}\dot{x}_i + a_{2i}\dot{x}_i^2 + f_{ri} + f_{ci} + f_{ti} \tag{5}$$

here a_{0i}, a_{1i}, and a_{2i} are the resistive coefficients for the ith vehicle, f_{ri} is the ramp resistance due to the track slope, f_{ci} is the curve resistance due to railway curvature, and f_{ti} is the tunnel resistance, all acting on the ith vehicle.

The traction/braking force considering the notch effect is

$$\Psi_i(F_i) = \begin{cases} F_i^{r\max}, & F_i > F_i^{rn} \\ k_i^{rj} F_i + \zeta_i^{rj}, & \begin{pmatrix} F_i^{r(j-1)} \le F_i \le F_i^{rj} \\ j = 2, \ldots, n \end{pmatrix} \\ k_i^{r1} F_i, & 0 \le F_i \le F_i^{r1} \\ k_i^{l1} F_i, & F_i^{l1} \le F_i \le 0 \\ k_i^{lj} F_i + \zeta_i^{lj}, & \begin{pmatrix} F_i^{lj} \le F_i \le F_i^{l(j-1)} \\ j = 2, \ldots, n \end{pmatrix} \\ F_i^{l\max}, & F_i < F_i^{ln} \end{cases} \tag{6}$$

where ζ_i^{rj} and ζ_i^{lj} $(i = 1, 2, \ldots, n;\ j = 2, \ldots, n)$ are the vertical intercept of the ith notch. They are zero when $F_i > F_i^{rn}$ and $F_i < F_i^{ln}$ as well as $0 \le F_i \le F_i^{r1}$ and $F_i^{l1} \le F_i \le 0$. It can be expressed generally as

$$\zeta_i = \begin{cases} 0, & F_i > F_i^{rn} \\ k_i^{rj}(-F_i^{r(j-1)}) + \sum_{h=1}^{j-1} \left[k_i^{rh} \left(F_i^{rh} - F_i^{r(h-1)} \right) \right], & \begin{pmatrix} F_i^{r(j-1)} \le F_i \le F_i^{rj} \\ j = 2, \ldots, n \end{pmatrix} \\ 0, & 0 \le F_i \le F_i^{r1} \\ 0, & F_i^{l1} \le F_i \le 0 \\ k_i^{lj}(-F_i^{l(j-1)}) + \sum_{h=1}^{j-1} \left[k_i^{lh} \left(F_i^{lh} - F_i^{l(h-1)} \right) \right], & \begin{pmatrix} F_i^{lj} \le F_i \le F_i^{l(j-1)} \\ j = 2, \ldots, n \end{pmatrix} \\ 0, & F_i < F_i^{ln} \end{cases}$$

where F_i is the variable to be designed, F_i^{rj} and F_i^{lj} are the neighboring notch values, and k_i^{rj} and k_i^{lj} are the slopes of the ith notch as shown in Fig. 2.

Remark 1: It should be emphasized that the in-train forces involved in the model are extremely difficult to model or measure precisely due to the nonlinear and elastic nature of the couplers connecting the vehicles. In most existing works, such in-train forces are either ignored or approximated with a linear model [12], [16]. In this paper, the in-train force of the form (4) is considered without linearization to better reflect the practical situation.

Remark 2: The model considered here is more effective in characterizing the dynamic behavior of a train as compared with the single point-mass model or multiple point-mass model with linear approximation commonly used in the literature.

B. Problem Statement

Let $X = [x_1, \ldots, x_n]^T$ be the displacement vector and $\dot{X} = [\dot{x}_1, \ldots, \dot{x}_n]^T$ be the velocity vector, the control objective is to design control force $F = [F_1, \ldots, F_n]^T$ so that for any given desired velocity–displacement $(\dot{X}^* - X^*)$ pair, we have $E \to 0$ and $\dot{E} \to 0$ as $t \to \infty$ or both E and $\dot{E}$ are uniformly ultimately confined within a small compact set containing the origin, where $E = X - X^*$ and $\dot{E} = \dot{X} - \dot{X}^*$ denote the position tracking error and velocity tracking error, respectively, $\dot{X}^*$ and X^* are the desired velocity and position, which, together with the desired acceleration $\ddot{X}^*$, are ensured to be smooth and bounded, produced from the train operation planning unit.

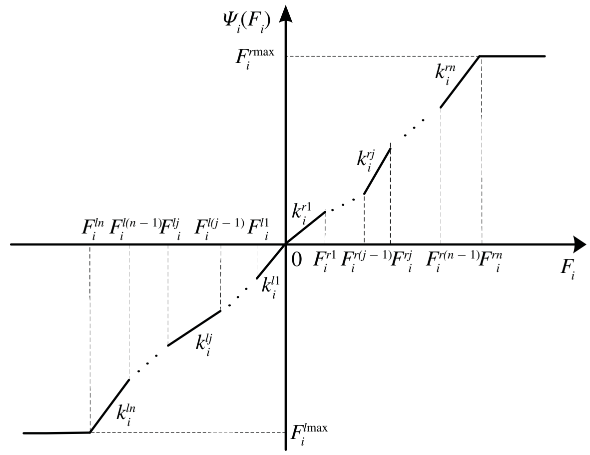

Fig. 2. Traction with rn notches and $F_i^{r\max}$ force limitation as well as braking with ln notches and $F_i^{l\max}$ force limitation.

The problem can be solved by using several existing methods [13]–[17] if m_i, f_{di}, and $g_i(\cdot)$ are available precisely. However, the mass of each vehicle of the train (m_i), the resistance coefficients $(a_{0i}$, a_{1i}, and $a_{2i})$, and other resistance $(f_{ri}$, f_{ci}, and $f_{ti})$ for each vehicle cannot be obtained accurately in practice, and some of them might even vary with operation conditions. Furthermore, even if those coefficients or resistance forces are obtainable, it is still a painful task to determine the in-train force $g_i(\cdot)$. The typical way to address this difficulty is to use the largely simplified linear/approximation model [12], [13], [15]–[17] for control design.

In this paper, we propose a solution to this problem by exploiting data-based neuroadaptive control method, in which no specific information on the total mass of the train, the resistance coefficients, or any other resistance forces is required. There is no need for precise measurement or computation of the in-train forces. Meanwhile, input nonlinearity and actuator failure are considered, as detailed in the following section.

III. Control Design and Stability Analysis

Note that (6) can be equivalently expressed as

$$\Psi_i(F_i) = \tau_i(\cdot) F_i + \zeta_i \tag{7}$$

where

$$\tau_i(\cdot) = \begin{cases} F_i^{r\max} / F_i, & F_i > F_i^{rn} \\ k_i^{rn}, & F_i^{r(n-1)} \le F_i \le F_i^{rn} \\ \vdots & \\ k_i^{r1}, & 0 \le F_i \le F_i^{r1} \\ k_i^{l1}, & F_i^{l1} \le F_i \le 0 \\ \vdots & \\ k_i^{ln}, & F_i^{ln} \le F_i \le F_i^{l(n-1)} \\ F_i^{l\max} / F_i, & F_i < F_i^{ln}. \end{cases}$$

Obviously, $|\zeta_i| \le \zeta_i^m < \infty$ for some constant $\zeta_i^m \ge 0$. For the traction and braking systems under consideration, there exist some positive constants $k_i^{l\min}$, $k_i^{l\max}$, $k_i^{r\min}$, and $k_i^{r\max}$ such that

$$0 < k_i^{l\min} \le k_i^{lj} \le k_i^{l\max}, \quad F_i^{lj} \le F_i \le F_i^{l(j-1)}$$
$$0 < k_i^{r\min} \le k_i^{rj} \le k_i^{r\max}, \quad F_i^{r(j-1)} \le F_i \le F_i^{rj}.$$

Therefore, it can be established that for all $F_i \in R$ there exists some constant $\tau_i^{\min} > 0$ such that $\tau_i^{\min} \le \tau_i$, $(i = 1, 2, \ldots, n)$. Then, we can get $0 < \tau_{\min} \le \tau_i(\cdot)$ $(i = 1, 2, \ldots, n)$, and $\tau_{\min} = \min\{\tau_1^{\min}, \ldots, \tau_i^{\min}, \ldots, \tau_n^{\min}\}$. For simple notation, we rewrite (3) as

$$M\ddot{X} = \Lambda\Psi(F) - F_d + (T - I)\, G_{in} \tag{8}$$
$$\Psi(F) = \tau(\cdot)\, F + \zeta \tag{9}$$

which, in light of (7), can be further expressed as

$$M\ddot{X} = \Lambda\Gamma F + \Upsilon_d(\cdot)$$
$$\Upsilon_d(\cdot) = \Lambda\zeta - F_d + (T - I)\, G_{in} \tag{10}$$

where $M = \mathrm{diag}(m_i)$, $\Lambda = \mathrm{diag}(\lambda_i)$, $\Gamma = \mathrm{diag}(\tau_i)$, $\zeta = \left[\zeta_1 \cdots \zeta_n\right]^T$, and $T = \begin{bmatrix} \mathbf{0}_{1\times(n-1)} & 1 \\ I_{(n-1)\times(n-1)} & \mathbf{0}_{(n-1)\times 1} \end{bmatrix}_{n\times n}$, with I being the identity matrix.

$F_d = [f_{d1}, f_{d2}, \ldots, f_{dn}]^T$ and $G_{in} = [g_1, g_2, \ldots, g_n]^T$ are the vectors of resistance and in-train forces, respectively, $\dot{X}$ is the velocity vector, $\ddot{X}$ is the acceleration vector, and Λ is the power/braking effectiveness distribution matrix.

To facilitate the control design and to arrange the relevant data for control operation, we define a filtered variable, S, in terms of tracking errors

$$S = \dot{E} + BE \tag{11}$$

with $B = \mathrm{diag}(\beta_i)$, where β_i is a free positive parameter chosen by the designer/user. Based on (11), we can re-express (10) as

$$M\dot{S} = \Lambda\Gamma F + L_d(\cdot) \tag{12}$$
$$L_d(\cdot) = \Lambda\zeta - F_d + (T - I)\, G_{in} - M\ddot{X}^* + MB\dot{E}. \tag{13}$$

Examining (35c) reveals that $L_d(\cdot)$ is nonlinear and unavailable precisely. In other words, the above dynamic model contains significant nonlinearities and uncertainties. Thus, it is highly desirable to develop a control scheme that does not rely on $L_d(\cdot)$ directly. The control schemes presented in the following section utilize the available "core" information of $L_d(\cdot)$, and NNs are employed online to approximate the nonlinear function. Note that NN has unique capabilities in approximating any nonlinear function with sufficient accuracy if the NN is constructed properly, and this feature has been widely used for coping with system nonlinearities and uncertainties [37]–[39]. There are some successful applications of NN in industrial systems [40], [41]. In this paper, three neuroadaptive control schemes are developed based on different treatments of $L_d(\cdot)$, with the first one to deal with the vector $L_d(\cdot)$ directly, the second one to cope with the norm bound on $L_d(\cdot)$, and the third one to accommodate $L_d(\cdot)$ and possible actuator faults, making use of the learning capability of NNs.

A. Neuroadaptive Control

As the first step, we reconstruct L_d via an NN unit as

$$L_d = W^T\Phi(z) + \kappa(z) \tag{14}$$

where $W = \begin{bmatrix} w_{11} & \cdots & w_{1l} \\ \vdots & \ddots & \vdots \\ w_{n1} & \cdots & w_{nl} \end{bmatrix}$ is the weight matrix, $\Phi(\cdot) = \left[\varphi_1(z) \cdots \varphi_l(z)\right]^T$ is the basis function vector, l is the number of neurons,$\kappa(\cdot) = \left[\varepsilon_1(\cdot) \cdots \varepsilon_n(\cdot)\right]^T$is the reconstruction error, and $z_i = \left[x_i, \dot{x}_i, x_{i+1}, \dot{x}_{i+1}, \ddot{x}_i^*, \dot{e}_i\right]^T$ $i = (1, 2, \ldots, n)$ (measurement noises are not considered in this paper). By the universal approximation theory, it is reasonable to assume that the NN reconstruction error $\|\kappa\| \le \varepsilon_0$, where ε_0 is an unknown positive constant.

Theorem 1: Consider the train dynamics with in-train force and traction/braking notches as described by (10). If the following control algorithm is applied

$$F = -\Lambda^T\left(k_0 S + \hat{W}^T\Phi - u_c\right) \tag{15a}$$
$$u_c = -\hat{a}\frac{\left(\left\|\hat{W}^T\Phi\right\| + 1\right)S}{\|S\|} \tag{15b}$$

with $\dot{\hat{W}} = \Phi S^T$, $\dot{\hat{a}} = \sigma_1\left(\left\|\hat{W}^T\Phi\right\| + 1\right)\left\|S\right\|$, where $\hat{a}$ is the estimation of a and $a = \max\{\left\|I - \Lambda\Gamma\Lambda^T\right\|,\ \varepsilon_0\}$, $\sigma_1 > 0$, $k_0 > 0$ are two free design parameters, then asymptotically stable position and velocity tracking are ensured.

Proof: With the proposed control (15), one gets the closed-loop error dynamic equation from (35a)

$$M\dot{S} = -k_0\Lambda\Gamma\Lambda^T S - \Lambda\Gamma\Lambda^T\hat{W}^T\Phi + \Lambda\Gamma\Lambda^T u_c + L_d(\cdot). \tag{16}$$

Using (35d), it is straightforward to get

$$M\dot{S} = -k_0\Lambda\Gamma\Lambda^T S + \tilde{W}^T\Phi + \Lambda\Gamma\Lambda^T u_c + \gamma_d(\cdot) \tag{17}$$

with

$$\gamma_d(\cdot) = \left(I - \Lambda\Gamma\Lambda^T\right)\hat{W}^T\Phi + \kappa \tag{18}$$

where

$$\tilde{W} = W - \hat{W}.$$

Let

$$a = \max\left\{\left\|I - \Lambda\Gamma\Lambda^T\right\|,\ \varepsilon_0\right\}$$

it is seen that

$$\|\gamma_d(\cdot)\| \le a\left(\left\|\hat{W}^T\Phi\right\| + 1\right). \tag{19}$$

Consider the Lyapunov function candidate

$$V = \frac{1}{2}S^T MS + \frac{tr\left(W - \hat{W}\right)^T\left(W - \hat{W}\right)}{2} + \frac{(a - \lambda_m\hat{a})^2}{2\lambda_m\sigma_1} \tag{20}$$

where $0 < \lambda_m \le \lambda_{\min}(\Lambda\Gamma\Lambda^T)$ and $\lambda_{\min} > 0$ is the minimum eigenvalue of $\Lambda\Gamma\Lambda^T$. Using (17), it follows that

$$\dot{V} = -k_0 S^T\Lambda\Gamma\Lambda^T S + S^T\tilde{W}^T\Phi + S^T\Lambda\Gamma\Lambda^T u_c + S^T\gamma_d + tr\left(W - \hat{W}\right)^T\left(-\dot{\hat{W}}\right) + (a - \lambda_m\hat{a})\frac{\left(-\dot{\hat{a}}\right)}{\sigma_1}. \tag{21}$$

Noting that $tr(S^T \tilde{W}^T \Phi) = tr(\tilde{W}^T \Phi S^T)$ and using the updating algorithms for $\hat{W}$ and $\hat{a}$ as well as the compensating unit u_c, one gets from (41c) that

$$\begin{aligned}\dot{V} &\leq -k_0\lambda_m \|S\|^2 + tr\tilde{W}^T\left(\Phi S^T - \dot{\hat{W}}\right) + \left(a - \lambda_m \hat{a}\right)\frac{\left(-\dot{\hat{a}}\right)}{\sigma_1} \\ &\quad -\lambda_m\hat{a}\left(\left\|\hat{W}^T\Phi\right\| + 1\right)\|S\| + a\left(\left\|\hat{W}^T\Phi\right\| + 1\right)\|S\| \\ &\leq -k_0\lambda_m\|S\|^2 \leq 0.\end{aligned}$$

Therefore, we have $V \in \ell_\infty$, which ensures that $S \in \ell_\infty$, $\hat{a} \in \ell_\infty$, and $\hat{W} \in \ell_\infty$, hence $\dot{E} \in \ell_\infty$, $E \in \ell_\infty$, $u_c \in \ell_\infty$, and $F \in \ell_\infty$. Then, it is readily shown that $\dot{S} \in \ell_\infty$, that is, S is uniformly continuous, which, together with the fact that $\int_0^\infty k_0\lambda_m \|S\|^2 \leq V(0) < \infty$, allows the Barbalat lemma to be used to conclude that $\lim_{t\to\infty} S = 0$, therefore $\dot{E} \to 0$, $E \to 0$ as $t \to \infty$ by the definition of S.

Remark 3: It should be pointed out that the estimation method of $\hat{a}$ as presented in Theorem 1 may cause parameter drift [42]. To avoid this problem, the following PI estimate algorithm is used to make suitable corrections [43].

Theorem 2: Assume the same conditions as in Theorem 1. Let the control scheme be the same as in (15), where $k_0 \geq (\sigma_0 a^2/2\sigma_1\lambda_m^2)$. If the following algorithm for $\hat{a}$ is used

$$\dot{\hat{a}} = -\sigma_0\|S\|^2\hat{a} + \sigma_1\left(\left\|\hat{W}^T\Phi\right\| + 1\right)\|S\| - \sigma_2\dot{\xi} \quad (22a)$$

$$\xi = \sigma_0\|S\|^2\hat{a} - \sigma_1\left(\left\|\hat{W}^T\Phi\right\| + 1\right)\|S\| \quad (22b)$$

where $\sigma_0 > 0$, $\sigma_1 > 0$, and $\sigma_2 > 0$ are design parameters. Then, asymptotically stable speed and position tracking are ensured.

Proof: To prove the result, we need to modify the Lyapunov function candidate (20b) to

$$V = \frac{1}{2}S^T M S + \frac{tr\left(W - \hat{W}\right)^T\left(W - \hat{W}\right)}{2} + \frac{(\tilde{a} + \lambda_m\sigma_2\xi)^2}{2\lambda_m\sigma_1} \quad (23)$$

where $\tilde{a} = \lambda_m\hat{a} - a$. Then, with (15a), (15b), (17), and (19), it is straightforward to show that

$$\begin{aligned}\dot{V} &\leq -k_0\lambda_m\|S\|^2 - \tilde{a}\left(\left\|\hat{W}^T\Phi\right\| + 1\right)\|S\| + S^T\tilde{W}^T\Phi \\ &\quad + tr\left(W - \hat{W}\right)^T\left(-\dot{\hat{W}}\right) + \frac{(\tilde{a} + \lambda_m\sigma_2\xi)\left(\dot{\hat{a}} + \sigma_2\dot{\xi}\right)}{\sigma_1}.\end{aligned} \quad (24)$$

Upon using the updating algorithms (22a) and (22b) and the fact that $tr(S^T\tilde{W}^T\Phi) = tr(\tilde{W}^T\Phi S^T)$, the terms $S^T\tilde{W}^T\Phi$ and $tr(W - \hat{W})^T(-\dot{\hat{W}})$ in (24) are cancelled out to arrive at

$$\begin{aligned}\dot{V} &\leq -k_0\lambda_m\|S\|^2 \\ &\quad -\tilde{a}\left(\left\|\hat{W}^T\Phi\right\| + 1\right)\|S\| + \frac{(\tilde{a} + \lambda_m\sigma_2\xi)\left(\dot{\hat{a}} + \sigma_2\dot{\xi}\right)}{\sigma_1} \\ &= -k_0\lambda_m\|S\|^2 - \tilde{a}\left(\left\|\hat{W}^T\Phi\right\| + 1\right)\|S\| + \tilde{a}\left(\left\|\hat{W}^T\Phi\right\| + 1\right)\|S\| \\ &\quad -\frac{\lambda_m\sigma_2\xi^2}{\sigma_1} - \frac{\sigma_0\|S\|^2\tilde{a}\hat{a}}{\sigma_1} \\ &\leq -k_0\lambda_m\|S\|^2 - \frac{\lambda_m\sigma_2\xi^2}{\sigma_1} - \frac{\sigma_0\|S\|^2\tilde{a}^2}{2\lambda_m\sigma_1} + \frac{\sigma_0\|S\|^2 a^2}{2\lambda_m\sigma_1} \\ &\leq -k_0\lambda_m\|S\|^2 + \frac{\sigma_0\|S\|^2 a^2}{2\lambda_m\sigma_1}\end{aligned} \quad (25)$$

where $-\tilde{a}\hat{a} \leq -(\tilde{a}^2/2\lambda_m) + (a^2/2\lambda_m)$ was used. It is then readily shown that $\dot{V} \leq 0$ if $k_0 \geq (\sigma_0 a^2/2\sigma_1\lambda_m^2)$. The result is established following the same argument as in the proof of Theorem 1.

Remark 4: It is noted that the proposed adaptation algorithm contains both integral and proportional terms. This PI estimate algorithm gives a better convergence property than using integral term alone.

B. Simplified Neuroadaptive Control

The previous neuroadaptive control scheme is based on using NN unit to deal with the lumped uncertain vector $L_d(\cdot)$ as defined in (35c) directly. As a parameter matrix (W) needs to be updated online in each approximator, heavy computation may be involved when the controlled system is of higher dimension. It is interesting to note that if the norm of $L_d(\cdot)$ is considered and the core data is mined from $L_d(\cdot)$, a simpler neuroadative control can be developed, as detailed in what follows.

First, with the assumption that the addition resistance f_{ri}, f_{ci}, and f_{ti} are bounded and a_{0i}, a_{1i}, and a_{2i} are unknown constants, it is readily shown that F_d in (13) can be bounded by $\|F_d\| \leq a_0 + a_1\left\|\dot{X}\right\| + a_3\left\|\dot{X}\right\|^2$ for some unknown constants a_0, a_1, and a_2. Second, the in-train force G_{in} involved in (13), although totally unavailable, satisfies

$$\begin{aligned}\|G_{in}\| &\leq \gamma\left(\Delta\dot{x}_{d1}, \Delta x_{d1}, \ldots, \Delta\dot{x}_{dn}, \Delta x_{dn}\right) \\ &\leq \phi(x_1, \ldots, x_n, \dot{x}_1, \ldots, \dot{x}_n)\end{aligned} \quad (26)$$

where $\phi(\cdot)$ is a nonlinear and scalar function of $\|X\|$ and $\left\|\dot{X}\right\|$. Thus, it holds that

$$\|(T - I)\,G_{in}\| \leq \eta_1\left(\|X\|, \left\|\dot{X}\right\|\right) \quad (27)$$

where $\eta_1(\cdot)$ is an unknown nonlinear continuous and scalar function. Third, with the assumption that X^*, $\dot{X}^*$, and $\ddot{X}^*$ are bounded and the fact that $\|\zeta\| \leq \zeta_m < \infty$, there exist some unknown and nonnegative constants l_1, l_2, and l_3 such that

$$\left\|\Lambda\zeta - F_d - M\ddot{X}^* + MB\dot{E}\right\| \leq \eta_2(\cdot) \quad (28a)$$

with

$$\eta_2\left(\left\|\dot{X}\right\|\right) = l_1 + l_2\left\|\dot{X}\right\| + l_3\left\|\dot{X}\right\|^2. \quad (28b)$$

Then, the lumped term L_d as defined in (13c) satisfies

$$\|L_d\| \leq \eta_1(\cdot) + \eta_2(\cdot). \quad (29)$$

It should be noted that $\eta_1(\cdot)$ and $\eta_2(\cdot)$ can be seen as the core information of $L_d(\cdot)$, and although $\eta_1(\cdot)$ and $\eta_2(\cdot)$ are still unknown, they are both scalar. We construct an adaptive control unit and an NN-based unit to deal with the unknown and scalar functions as follows

$$\eta_1(\cdot) = w^T\varphi(z) + \varepsilon(z) \ \text{ and } \ \hat{\eta}_2(\cdot) = \hat{l}_1 + \hat{l}_2\|\dot{X}\| + \hat{l}_3\|\dot{X}\|^2 \tag{30}$$

where $\hat{l}_1$, $\hat{l}_2$, and $\hat{l}_3$ are the estimation of l_1, l_2, and l_3, $w \in R^p$ is the weight vector (not matrix) and $\varphi(z) \in R^p$ is the basic function with $z = [\|X\|, \|\dot{X}\|]^T$ being the NN input, and $\varepsilon(z) \in R$ is the NN approximation error. Since the NN is used to cope with the scalar (rather than vector) unknown function, the corresponding control scheme turns out to be much simpler, as seen from the following development.

Theorem 3: Consider the train with the dynamics as given by (10). Assume that the approximation error $|\varepsilon| \le \varepsilon_m < \infty$, where ε_m is an unknown constant. If the following NN-based robust adaptive control law is applied

$$F = -k_0\Lambda^T S + u_a + u_b + u_c \tag{31a}$$

$$u_a = -\Lambda^T\left(\hat{l}_1 + \hat{l}_2\|\dot{X}\| + \hat{l}_3\|\dot{X}\|^2\right)\frac{S}{\|S\|} \tag{31b}$$

$$u_b = -\Lambda^T\hat{w}^T\varphi\frac{S}{\|S\|} \tag{31c}$$

and

$$u_c = -\Lambda^T\hat{\varepsilon}_m\frac{S}{\|S\|} \tag{31d}$$

with

$$\dot{\hat{w}} = \|S\|\varphi, \quad \dot{\hat{\varepsilon}}_m = \sigma_1\|S\| \tag{32a}$$

$$\dot{\hat{l}}_1 = \sigma_{l1}\|S\|, \quad \dot{\hat{l}}_2 = \sigma_{l2}\|S\|\|\dot{X}\|, \quad \dot{\hat{l}}_3 = \sigma_{l3}\|S\|\|\dot{X}\|^2 \tag{32b}$$

where $\sigma_1 > 0$, $\sigma_{l1} > 0$, $\sigma_{l2} > 0$, and $\sigma_{l3} > 0$ are some free design parameters, $\hat{\varepsilon}_m$ is the estimation of ε_m. Then, asymptotically position and velocity tracking are ensured.

Proof: In view of (12) and (31a), we get

$$M\dot{S} = -k_0\Lambda\Gamma\Lambda^T S + \Lambda\Gamma u_a + \Lambda\Gamma u_b + \Lambda\Gamma u_c + L_d(\cdot). \tag{33}$$

Define $\tilde{\varepsilon}_m = \varepsilon_m - \lambda_m\hat{\varepsilon}_m$, $\tilde{w} = w - \lambda_m\hat{w}$, $\tilde{l}_1 = l_1 - \lambda_m\hat{l}_1$, $\tilde{l}_2 = l_2 - \lambda_m\hat{l}_2$, and $\tilde{l}_3 = l_3 - \lambda_m\hat{l}_3$. Note that the parameter/weight estimate errors are defined not as the direct discrepancy between the actual and the estimate values, such treatment allows for the following Lyapunov function candidate to be constructed

$$V = \frac{1}{2}S^T MS + \frac{\tilde{\varepsilon}_m^2}{2\lambda_m\sigma_1} + \frac{\tilde{l}_1^2}{2\lambda_m\sigma_{l1}} + \frac{\tilde{l}_2^2}{2\lambda_m\sigma_{l2}} + \frac{\tilde{l}_3^2}{2\lambda_m\sigma_{l3}} + \frac{\tilde{w}^T\tilde{w}}{2\lambda_m} \tag{34}$$

where $\lambda_m > 0$ is defined as before (i.e., the minimum eigenvalue of $\Lambda\Gamma\Lambda^T$). It can be shown with the control algorithms (31a) and (32b) that

$$\begin{aligned}\dot{V} &= S^T M\dot{S} + \tilde{\varepsilon}_m\left(\frac{-\dot{\hat{\varepsilon}}_m}{\sigma_1}\right) + \tilde{l}_1\left(\frac{-\dot{\hat{l}}_1}{\sigma_{l1}}\right) + \tilde{l}_2\left(\frac{-\dot{\hat{l}}_2}{\sigma_{l2}}\right) \\ &\quad + \tilde{l}_3\left(\frac{-\dot{\hat{l}}_3}{\sigma_{l3}}\right) + \tilde{w}^T\left(-\dot{\hat{w}}\right) \\ &\le -k_0\lambda_m\|S\|^2 - \lambda_m\left(\hat{l}_1 + \hat{l}_2\|\dot{X}\| + \hat{l}_3\|\dot{X}\|^2\right)\|S\| \\ &\quad -\lambda_m\|S\|\hat{w}^T\varphi - \lambda_m\hat{\varepsilon}_m\|S\| + \|S\|\left(l_1 + l_2\|\dot{X}\| + l_3\|\dot{X}\|^2\right) \\ &\quad + \|S\|w^T\varphi + \|S\|\varepsilon_m + \tilde{l}_1(-\|S\|) + \tilde{l}_2\left(-\|S\|\|\dot{X}\|\right) \\ &\quad + \tilde{l}_3\left(-\|S\|\|\dot{X}\|^2\right) + \tilde{w}^T(-\|S\|\varphi) - \tilde{\varepsilon}_m\|S\| \\ &\le -k_0\lambda_m\|S\|^2 \le 0.\end{aligned}$$

The result is then established using the same argument as in the proof of Theorem 1.

It is interesting to note that the control scheme can be further simplified by treating the upper bound of w and ε as a single unknown parameter for estimation, as stated in the following Corollary.

Corollary 1: Consider the train dynamics as given by (10). Let the following neuroadaptive robust adaptive control scheme be implemented

$$F = -k_0\Lambda^T S + u_a + u_c \tag{35a}$$

$$u_a = -\Lambda^T\left(\hat{l}_1 + \hat{l}_2\|\dot{X}\| + \hat{l}_3\|\dot{X}\|^2\right)\frac{S}{\|S\|} \ \text{ and}$$

$$u_c = -\Lambda^T\hat{\rho}\frac{(\|\varphi\| + 1)S}{\|S\|} \tag{35b}$$

where $k_0 > 0$ is a free control parameter, $\hat{\rho}$ is the estimate of $\rho = \max\{\|w\|, |\varepsilon|\}$, which is updated by

$$\dot{\hat{\rho}} = \sigma_1(\|\varphi\| + 1)\|S\| \tag{35c}$$

and

$$\dot{\hat{l}}_1 = \sigma_{l1}\|S\|, \quad \dot{\hat{l}}_2 = \sigma_{l2}\|S\|\|\dot{X}\|, \quad \dot{\hat{l}}_3 = \sigma_{l3}\|S\|\|\dot{X}\|^2 \tag{35d}$$

where $\sigma_1 > 0$, $\sigma_{l1} > 0$, $\sigma_{l2} > 0$, and $\sigma_{l3} > 0$ are parameters chosen by the designer. Then, asymptotically stable position and velocity tracking are ensured.

Proof: In view of (12) and (35a), the closed error dynamics are

$$M\dot{S} = -k_0\Lambda\Gamma\Lambda^T S + \Lambda\Gamma u_a + \Lambda\Gamma u_c + L_d(\cdot). \tag{36}$$

Modify the Lyapunov function candidate (34) as

$$V = \frac{1}{2}S^T MS + \frac{(\rho - \lambda_m\hat{\rho})^2}{2\lambda_m\sigma_1} + \frac{\tilde{l}_1^2}{2\lambda_m\sigma_{l1}} + \frac{\tilde{l}_2^2}{2\lambda_m\sigma_{l2}} + \frac{\tilde{l}_3^2}{2\lambda_m\sigma_{l3}}. \tag{37}$$

It can be shown with the control algorithms (35a) and (35d) that

$$\begin{aligned}\dot{V} &\le -k_0\lambda_m\|S\|^2 - \lambda_m\hat{\rho}\|S\|(\|\varphi\| + 1) + \rho\|S\|(\|\varphi\| + 1) \\ &\quad - (\rho - \lambda_m\hat{\rho})(\|\varphi\| + 1)\|S\| \le -k_0\lambda_m\|S\|^2 \le 0.\end{aligned}$$

Then, the result is established using the same argument as in the proof of Theorem 1.

C. Neuroadaptive Fault-Tolerant Control

As actuation faults may occur during the system operation, it is important to address the fault-tolerant control issue explicitly. Here, we consider the situation that the powering unit or braking unit (called "actuator" hereafter) of some vehicle fails to work properly in that actuation/braking capabilities are fading. The fault-tolerant control objective here is to maintain safe operation and avoid any possible operation accident whenever a failure occurs. Note that in such situation, the actual traction/braking force F_a and the designed traction/braking force F are not identical anymore, instead, they are related through

$$F_a = \gamma F + \Re(\cdot) \tag{38}$$

where $\|\Re(\cdot)\| \le r_c < \infty$ is the uncertain partition of the control caused by the actuator failure, $\gamma(\cdot) = \mathrm{diag}\{\gamma_1(\cdot), \gamma_2(\cdot), \ldots, \gamma_n(\cdot)\}$ is a diagonal matrix of powering and braking effectiveness, with $0 \le \gamma_i(\cdot) \le 1$ being the "powering/braking health indicator" [43] for the ith vehicle. The case of $\gamma_i(\cdot) = 0$ implies that the ith vehicle totally loses its traction or braking capability, $0 < \gamma_i(\cdot) < 1$ corresponds to the case that the ith vehicle partially loses its traction or braking effectiveness; and $\gamma_i(\cdot) = 1$ implies that the powering/braking system of the ith vehicle is healthy and functioning normally.

In order for the system to admit a feasible control solution, one must assume that the remaining functional actuators are able to generate sufficient power to move forward or stop the train whenever it is necessary. To address the control design problem, we consider the case that some or all actuators suffer from partial actuation failures, that is, $0 < \gamma_i(\cdot) < 1$ $(i = 1, \ldots, n)$. Note that $\gamma(\cdot)$ is a diagonal but uncertain actuation effectiveness matrix.

Now, we develop a neuroadaptive fault-tolerant control to cope with the actuation faults and the uncertain in-train forces as well as the nonsymmetric input nonlinearities. To this end, we combine (12), (13), and (38) to get the closed-loop error dynamics

$$M\dot{S} = \Lambda\Gamma\gamma F + L_d(\cdot) \tag{39}$$

$$\begin{aligned} L_d(\cdot) &= \Lambda\Gamma\Re(\cdot) + \Lambda\zeta - F_d + (T - I)G_{\text{in}} \\ &\quad - M\ddot{X}^* + MB\dot{E}. \end{aligned} \tag{40}$$

The idea is to use an NN unit of the form $W^T\Phi$ to counteract the lumped uncertain term $L_d(\cdot)$ and incorporate a robust unit to compensate the NN reconstruction error $\|\kappa\| \le \varepsilon_0 < \infty$. This leads to the following result.

Theorem 4: Consider the train with actuation faults satisfying the condition as imposed in (38). If the control force F is designed as in (41a) and (42b), then asymptotic velocity and position tracking are achieved.

$$F = -\Lambda^T\left(k_0 S + \hat{W}^T\Phi - u_c\right) \tag{41a}$$

$$u_c = -\hat{a}\frac{\left(\left\|\hat{W}^T\Phi\right\| + 1\right)S}{\|S\|} \tag{41b}$$

where

$$\dot{\hat{W}} = \Phi S^T \tag{41c}$$

$$\dot{\hat{a}} = \sigma_1\left(\left\|\hat{W}^T\Phi\right\| + 1\right)\|S\| \tag{42a}$$

or

$$\begin{aligned} \dot{\hat{a}} &= -\sigma_0\|S\|^2\hat{a} + \sigma_1\left(\left\|\hat{W}^T\Phi\right\| + 1\right)\|S\| - \sigma_2\dot{\xi} \\ \xi &= \sigma_0\|S\|^2\hat{a} - \sigma_1\left(\left\|\hat{W}^T\Phi\right\| + 1\right)\|S\|. \end{aligned} \tag{42b}$$

Proof: With the proposed control (41), the closed-loop error dynamics become

$$M\dot{S} = -k_0\Lambda\Gamma\gamma\Lambda^T S - \Lambda\Gamma\gamma\Lambda^T\hat{W}^T\Phi + \Lambda\Gamma\gamma\Lambda^T u_c + L_d(\cdot). \tag{43}$$

Using the NN unit, the lumped uncertain term $L_d(\cdot)$ is now replaced by $W^T\Phi(z) + \kappa(z)$. As a result, (43) can be readily expressed as

$$M\dot{S} = -k_0\Lambda\Gamma\gamma\Lambda^T S + \tilde{W}^T\Phi + \Lambda\Gamma\gamma\Lambda^T u_c + \gamma_d(\cdot) \tag{44}$$

with

$$\gamma_d(\cdot) = \left(I - \Lambda\Gamma\gamma\Lambda^T\right)\hat{W}^T\Phi + \kappa \tag{45}$$

where

$$\tilde{W} = W - \hat{W}.$$

Let

$$a = \max\{\left\|I - \Lambda\Gamma\gamma\Lambda^T\right\|,\ \varepsilon_0\}$$

it holds that

$$\|\gamma_d(\cdot)\| \le a\left(\left\|\hat{W}^T\Phi\right\| + 1\right). \tag{46}$$

Consider the Lyapunov function candidate

$$V = \frac{1}{2}S^T MS + \frac{tr\left(W - \hat{W}\right)^T\left(W - \hat{W}\right)}{2} + \frac{(a - \lambda_m\hat{a})^2}{2\lambda_m\sigma_1} \tag{47}$$

where $0 < \lambda_m \le \lambda_{\min}(\Lambda\Gamma\gamma\Lambda^T)$ and $\lambda_{\min} > 0$ is the minimum eigenvalue of $\Lambda\Gamma\gamma\Lambda^T$. The rest of the proof follows the same lines as in the proof of Theorem 1 [if the update algorithms (41c) and (42a) are used] or Theorem 2 [if the update algorithms (41c) and (42b) are used].

It is interesting to note that without any modification to the control scheme in Corollary 1, stable fault-tolerant tracking control can also be ensured, as stated in Corollary 2.

Corollary 2: Let F be the same as in Corollary 1, that is

$$F = -k_0\Lambda^T S + u_a + u_c \tag{48a}$$

$$u_a = -\Lambda^T\left(\hat{l}_1 + \hat{l}_2\left\|\dot{X}\right\| + \hat{l}_3\left\|\dot{X}\right\|^2\right)\frac{S}{\|S\|} \tag{48b}$$

$$u_c = -\Lambda^T\hat{\rho}\frac{(\|\varphi\| + 1)S}{\|S\|} \tag{48c}$$

with

$$\dot{\hat{\rho}} = \sigma_1(\|\varphi\| + 1)\|S\| \tag{48d}$$

$$\begin{aligned} \dot{\hat{l}}_1 &= \sigma_{l1}\|S\|, \quad \dot{\hat{l}}_2 = \sigma_{l2}\|S\|\left\|\dot{X}\right\|, \\ \dot{\hat{l}}_3 &= \sigma_{l3}\|S\|\left\|\dot{X}\right\|^2. \end{aligned} \tag{48e}$$

The control parameters are defined as before. Then, asymptotically stable speed and position tracking are ensured in the presence of actuation faults.

The result can be established by using the same form of Lyapunov function as in Corollary 1 in which the parameter

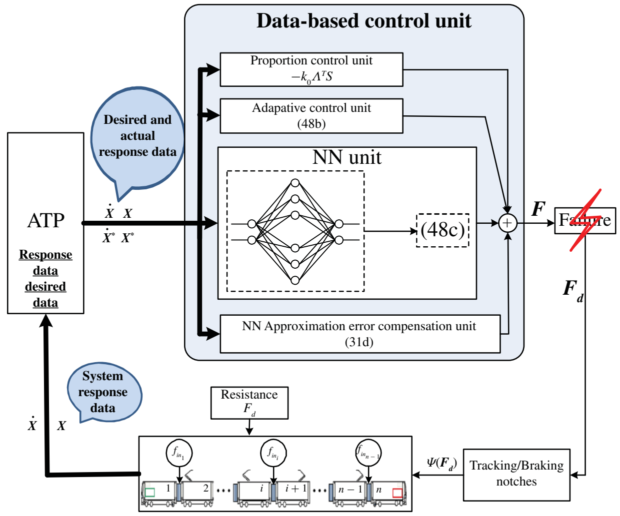

Fig. 3. Block diagram of the proposed control scheme (48) driven by data sets $\{\dot{X}^*, X^*, \dot{X}$ and $X\}$.

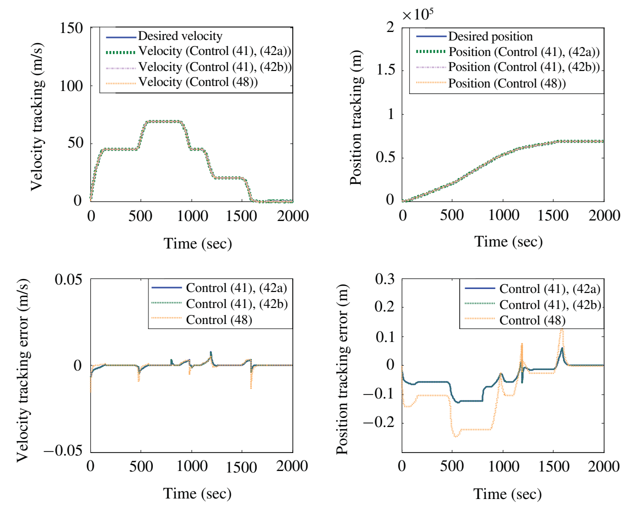

Fig. 4. Velocity and position tracking process and errors.

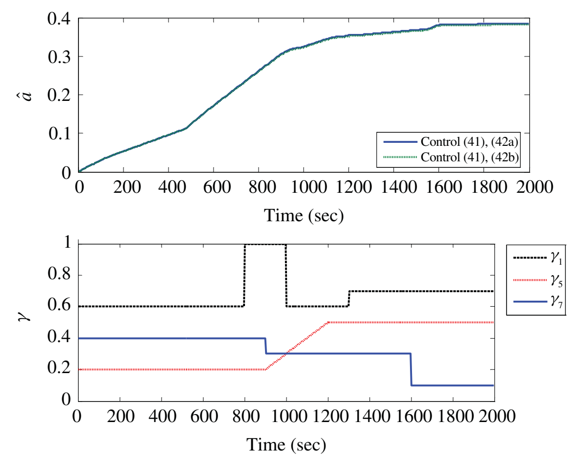

Fig. 5. Estimation of $\hat{a}$ and the actuation effectiveness.

$\lambda_m > 0$ (used for stability but not involved in the algorithms) is defined as $0 < \lambda_m \leq \min\left[\text{eigenvalue of}\{\Lambda\Gamma\gamma\Lambda^T\}\right]$–note that such $\lambda_m > 0$ does exist because the matrix $\Lambda\Gamma\gamma\Lambda^T$ is symmetric and positive definite for all the possible actuation failures $0 < \gamma_i(\cdot) < 1 \quad (i = 1, \ldots, n)$.

The block diagram of the overall control scheme (48) is depicted in Fig. 3, from which we can observe that as long as the input-response data sets $\{\dot{X}^*, X^*, \dot{X}$, and $X\}$ are available (the desired velocity and position are obtained through the train operation unit), the control algorithms can automatically generate $u_a, \hat{l}_1, \hat{l}_2, \hat{l}_3$, and $\hat{\rho}$, and so on, and eventually produce the traction/braking force F without the need for precise system model or system parameters, nor human intervention. As such, the proposed control is primarily a class of data-driven control.

D. Radial Basis Function and (RBF) NNs

RBF NNs are popular for their simplicity, fast learning, and universal approximation properties [22]. The construction of the RBF NNs involves three different layers: 1) input layer that consists of input nodes; 2) hidden layer where each neuron computes its activation using RBF; and 3) output layer that builds a linear weighted sum of hidden-layer activations to output the response of the network. The analytic expression of the activation of an RBF with different widths adopted in this paper can be written as

$$\varphi_k(\cdot) = \exp\left(-\sum_{j=1}^{q}\left(z_j - c_{kj}\right)^2 \Big/ 2\sigma_{kj}^2\right) \quad (k = 1, 2, \ldots, N)$$

where $Z = \left[z_1, \ldots, z_q\right]^T$ is the input vector of NN. $C_{kj} = \left[c_{k1}, \ldots, c_{kq}\right]^T$ and $Q_{kj} = \left[\sigma_{k1}, \ldots, \sigma_{kq}\right]^T$ are the center states and standard deviations of Gaussian associated with each element of the input vector, respectively, and N is the number of hidden-layer neurons.

Remark 5: The control algorithms developed in this paper do not need the precise information of system parameters, nonlinear in-train force, the powering and braking effectiveness of the actuators (γ), resistance coefficients (a_{0i}, a_{1i}, a_{2i}), and other resistance (f_{ri}, f_{ci}, f_{ti}).

Remark 6: It is noted that the control schemes involve the switch function $(S/\|S\|)$, which might cause chattering as $\|S\|$ approaches to zero. A simple and effective solution is to replace it with $(S/\|S\| + \Delta(\cdot))$, where $\Delta(\cdot)$ is a small constant. Then, uniformly ultimately bounded (UUB) velocity and position tracking error are ensured.

Remark 7: Two types of control design parameters are involved in the proposed control method and none of them requires manual consistent tuning–some of the parameters can be chosen by the designer quite arbitrarily and the rest are automatically updated (adjusted) by the algorithms provided. Analysis on how sensitively the control performance depends on those design parameters (out of the scope of current paper, though) represents an interesting topic for future work (Table I).

IV. Simulation

To test the performance of the proposed control strategies, simulation tests are carried out on a train similar to CRH-5

TABLE I

CONTROL STRATEGIES

Control system	Scheme	Parameter estimation strategies	Input of NN
I	$F = \Lambda^T(k_0 S + \hat{W}^T\Phi - u_c)$ $u_c = -\hat{a}\frac{(\Vert\hat{\omega}^T\Phi\Vert+1)S}{\Vert S\Vert}$	$\dot{\hat{a}} = \Phi S^T$ $\dot{\hat{a}} = \sigma_1\left(\Vert\hat{\omega}^T\Phi\Vert + 1\right)\Vert S\Vert$ **or** $\dot{\hat{a}} = -\sigma_0\Vert S\Vert^2\hat{a} - \sigma_2\dot{\xi}$ $+\sigma_1\left(\Vert\hat{W}^T\Phi + 1\right)\Vert S\Vert$ $\xi = -\sigma_1\left(\Vert\check{W}^T\Phi + 1\right)\Vert S\Vert$ $+\sigma_0\Vert S\Vert^2\hat{a}$	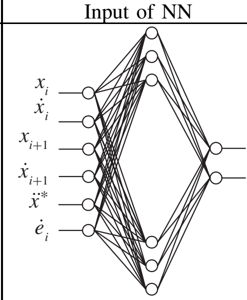 the ith NN (i = 1,2, ... n),
II	$F = -K\Lambda_0^T S + u_a + u_b + u_c$ $u_a = -\Lambda^T\hat{l}_1\frac{s}{\Vert S\Vert} + \hat{l}_2\Vert\dot{X}\Vert\frac{S}{\Vert S\Vert}$ $+\hat{l}_3\Vert\dot{X}\Vert^2\frac{S}{\Vert S\Vert}$ $u_b = -\Lambda^T\hat{\omega}^T\phi\}\frac{S}{S}\Vert$ $u_c = -\Lambda^T\hat{\varepsilon}_m\frac{S}{\Vert S\Vert}$	$\dot{\hat{W}} = \Vert S\Vert\phi$ $\dot{\hat{\xi}}_m = \sigma_1\Vert S\Vert$ $\dot{\hat{l}}_1 = \sigma_{l1}\Vert S\Vert$ $\dot{\hat{l}}_2 = \sigma_{l2}\Vert S\Vert\Vert\dot{X}\Vert$ $\dot{\hat{l}}_3 = \sigma_{l3}\Vert S\Vert\Vert\dot{X}\Vert^2$	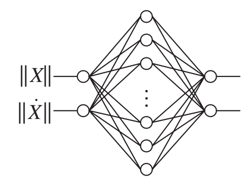 Only one NN is needed
III	$F = -K_0\Lambda^T S + u_0 + u_c$ $u_a = -\Lambda^T(\hat{l}_1 + \hat{l}_2\Vert\dot{X}\Vert$ $+\hat{l}_3\Vert\dot{X}\Vert^2)\frac{S}{\Vert S\Vert}$ $u_c = -\Lambda^T\hat{\rho}\frac{(\Vert\phi\Vert+1)S}{\Vert S\Vert}$	$\dot{\hat{\rho}} = \sigma_1(\Vert\phi\Vert + 1)\Vert S\Vert\dot{\hat{l}}_i = \sigma_{l1}\Vert S\Vert$ $\dot{\hat{l}}_2 = \sigma_{l2}\Vert S\Vert\dot{X}\Vert\dot{\hat{l}}_3 = \sigma_{l3}\Vert S\Vert\Vert\dot{X}\Vert^2$ or $\dot{\hat{\rho}} = -\sigma_0\Vert S\Vert^2\hat{\rho} + \sigma_1(\Vert\phi\Vert +$ $1)\Vert S\Vert - \sigma_2\hat{\xi}$ $\dot{\hat{l}}_1 = -\sigma'_{l1}\Vert S\Vert^2\hat{l}_1 + \sigma_{l1}\Vert S\Vert - \sigma''_{l1}\hat{\xi}_1$ $\xi_1 = \sigma'_{l1}\Vert S\Vert^2\hat{l}_1 - \sigma_{l1}\Vert S\Vert$ $\dot{\hat{l}}_2 = -\sigma'_{l2}\Vert S\Vert^2\hat{l}_2 + \sigma_{l2}\Vert S\Vert\Vert\dot{X}\Vert$ $-\sigma''_{l2}\hat{\xi}_2$ $\xi_2 = \sigma'_{l2}\Vert S\Vert^2\hat{l}_2 - \sigma_{l2}\Vert S\Vert\Vert\dot{X}\Vert$ $\dot{\hat{l}}_3 = -\sigma'_{l3}\Vert S\Vert^2\hat{l}_3 + \sigma_{l3}\Vert S\Vert\Vert\dot{X}\Vert^2$ $-\sigma''_{l3}$ $\xi_3 = \sigma'_{l3}\Vert S\Vert^2\hat{l}_3 - \sigma_{l3}\Vert S\Vert\Vert\dot{X}\Vert^2$	

TABLE II

PARAMETERS OF THE VEHICLES

Description	Value			
m_i The total mass of the i^{th} vehicle	$m_i = (50 + \Delta m_i)(ton)\ \Delta m_i \in [-7, 13]$			
a_{0i}, a_{li}, a_{2i} The resistance coefficients	$a_{0i} \in$ [50, 85] $a_{li} \in$ [30, 100] $a_{2i} \in$ [0.1, 6.5]			
Λ The power/breaking effectiveness distribution matrix	$\lambda = diag$([0.50.10.70.30.60.20.60.4])			
γ The diagonal matrix of powering and breaking effectiveness (three vehicles suffer from lost of effectiveness, and the others are healthy)	γ_i / Time (sec)	$\gamma 1$	$\gamma 5$	$\gamma 2$
	$t \in$ [0, 800]	0.6	0.2	0.4
	$t \in$ [800, 900]	1	0.2	0.4
	$t \in$ [1000, 1200]	1	(t–900)/1000+ 0.2	0.3
	$t \in$ [1200, 1300]	0.6	(t–900)/1000+ 0.2	0.3
	$t \in$ [200, 1300]	0.6	0.5	0.3
	$t \in$ [1200, 1600]	0.7	0.5	0.3
	$t \in$ [1600, 200]	0.7	0.5	0.1

with eight vehicles (i.e., four locomotives with both motoring and braking capabilities and four carriages with braking capabilities). The parameters used for simulation are listed in Table II.

Basis function of Gaussian sum nets is given by $\varphi_k(\cdot) = \prod_{j=1}^{q}\exp(-(z_j - c_{kj})^2/2\sigma_{kj}^2)(k = 1, 2, \ldots, N)$, where $Z = [z_1, \ldots, z_q]^T$ is the input vector of NN, $C_{kj} = [c_{k1}, \ldots, c_{kq}]^T$ and $Q_{kj} = [\sigma_{k1}, \ldots, \sigma_{kq}]^T$ are the center states and standard deviations of Gaussian associated with each element of the input vector, respectively. In the simulation, the number of hidden-layer neurons $N$for each subnet is chosen as 10. The connecting weights are all initialized at zero. Recall the description in Table I, the input vector of each NN is $z_i = [x_i,\ \dot{x}_i,\ x_{i+1},\ \dot{x}_{i+1},\ \ddot{x}_i^*,\ \dot{e}_i]^T$ in the first set of control scheme, so the center states, c_{k1}, c_{k2}, c_{k3}, c_{k4}, c_{k5}, and c_{k6} are set over the range [0, 0.1], [−0.1, 0.1], [−0.5, 0.5], [1, 2],

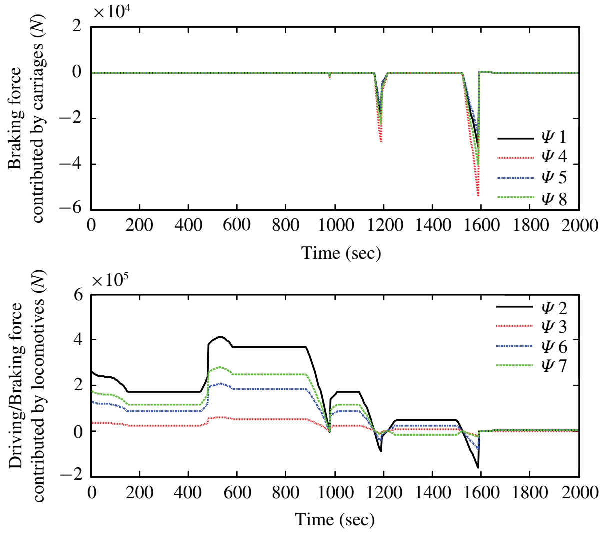

Fig. 6. Actual driving/braking force [control (41) and (42a)].

TABLE III
OPERATION CONDITIONS

Opertion Condition / Times (sec)	Curve radius (meter)	Slope (degree)	Tunnel force (N)
$t \in [200, 400]$	—	25	—
$t \in [600, 750]$	300	30	676.89 $\sin(0.1t)\sin(0.2t)$
$t \in [1400, 1570]$	300	—	—

[0.5, 1], and [0.1, 0.2], respectively, for each subnets. The standard deviation is set to be $\sqrt{2}$. For the second and third control schemes, c_{k1} and c_{k2} are set over the range as before. Similar simulation results are obtained (not presented here due to space constraint) with different choices for the width and number of neurons.

The travel distance tested in the simulation is 68.958 km, which covers two acceleration phases, four cruise phases, and three braking phases. The operation conditions are shown as in Table III. The goal is to make the actual velocity $\dot{x}$ and position x track the desired velocity $\dot{x}^*$and desired position x^* with high precision, respectively.

The design parameters of the controller can be set quite arbitrarily without the need for consistently tuning by the designer for tracking stability, although some trade-off is needed to accommodate the tracking precision and the magnitude of the control effort.

With three fading actuators (motor 1, motor 5, and motor 7), the fault-tolerant control algorithms (41), (42), and (48) are tested and the results are presented in Figs. 4–8. From Fig. 4, one can observe that the proposed neuroadaptive fault-tolerant control scheme performs well even if some of the actuators lose their effectiveness during the system operation.

The force F in (15), (31), (41), and (48) represents the total (combined) driving/braking force contributed by each power engine and braking system. If the vehicle is a locomotive, it provides both traction and braking forces. If the vehicle is a carriage, it provides only braking force. As shown in Figs. 6–8, in the acceleration and cruise phases, the locomotives produce traction force and the braking system has no contribution to the traction force, whereas when the train is in the braking phase, the motor unit outputs zero traction force, whereas the braking unit produces the braking force, which agrees with the theoretical prediction and practical setting.

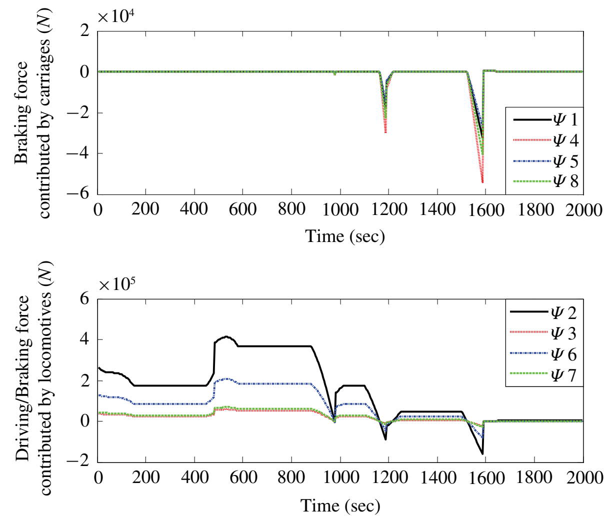

Fig. 7. Actual driving/braking force [control (41) and (42b)].

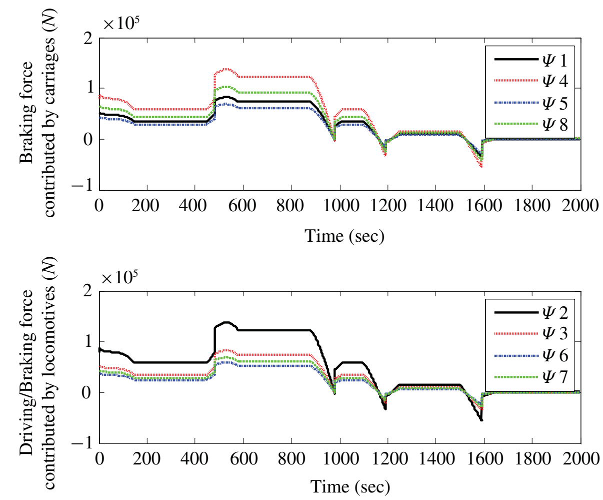

Fig. 8. Actual driving/braking force [control (48)].

Remark 8: It should be mentioned that with the actuation faults and input nonlinearities as well as modeling uncertainties as described in the train model, the typical model-based or adaptive control (either linear or nonlinear) is inapplicable, as verified in our simulation, where the UUB tracking error is no longer ensured under the aforementioned anomaly conditions (not shown here due to page limit).

V. CONCLUSION

The problem of speed and position tracking control of high-speed trains with multiple vehicles was studied in this paper. Input nonlinearities, actuator failures, and in-train forces were considered explicitly in control design. Several data-based fault-tolerant control algorithms were developed based on Lyapunov stability theory. The salient feature of the proposed control lies in its independence of precise system model/parameters and its simplicity in design as well as its effectiveness in dealing with various uncertainties and nonlinearities or even actuation faults. The proposed control is essentially data based in that the traction/braking control action can be generated automatically with the related system input-response data–there is no need for precise system model, accurate system parameters, or complicated and time-consuming design procedure.

REFERENCES

[1] H. Liu, X. Zhang, and W. Chang, "PID control of Maglev train system," in *Proc. Int. Conf. Ind. Inf. Syst.*, Changsha, China, Apr. 2009, pp. 341–343.

[2] S. Yansunobu, S. Miyamoto, and H. Ihara, "A fuzzy control for train automatic stop control," *Trans. Soc. Instrum. Control Eng.*, vol. E-2, no. 1, pp. 1–9, 2002.

[3] Q. Song, Y. D. Song, and W. Cai, "Adaptive backstepping control of train systems with traction/braking dynamics and uncertain resistive forces," *Veh. Syst. Dyn.*, vol. 49, no. 9, pp. 1441–1454, 2011.

[4] Q. Song and Y. D. Song, "Robust and adaptive control of high speed train systems," in *Proc. 22th Chin. Control Decis. Conf.*, Xuzhou, China, May 2010, pp. 2469–2474.

[5] P. Howlett, "Optimal strategies for the control of a train," *Automatica*, vol. 32, no. 4, pp. 519–532, Apr. 1996.

[6] E. Khmelnitsky, "On an optimal control problem of train operation," *IEEE Trans. Autom. Control*, vol. 45, no. 7, pp. 1257–1266, Jul. 2000.

[7] R. Liu and I. M. Golovitcher, "Energy-efficient operation of rail vehicles," *Transport. Res. Part A: Policy Pract.*, vol. 37, no. 10, pp. 917–932, 2003.

[8] J. Guzinski, H. Abu-Rub, M. Diguet, Z. Krzeminski, and A. Lewicki, "Application of speed and load torque observers in high-speed train drive for diagnostic purpose," *IEEE Trans. Ind. Electron.*, vol. 56, no. 1, pp. 248–256, Jan. 2009.

[9] J. P. Xu and J. P. Wang, "Bi-frequency pulse-train control technique for switching DC-DC converters operating in DCM," *IEEE Trans. Ind. Electron.*, vol. 58, no. 8, pp. 3658–3667, Aug. 2011.

[10] J. Guzinski, H. Abu-Rub, M. Diguet, Z. Krzeminski, and A. Lewicki, "Speed and load torque observer application in high-speed train electric drive," *IEEE Trans. Ind. Electron.*, vol. 57, no. 2, pp. 565–574, Feb. 2010.

[11] J.-W. Kim, J.-S. You, and B. H. Cho, "Modeling, control, and design of input-series-output-parallel-connected converter for high-speed-train power system," *IEEE Trans. Ind. Electron.*, vol. 48, no. 3, pp. 536–544, Jun. 2001.

[12] C. Yang and Y. Sun, "Robust cruise control of high speed train with hardening/softening nonlinear coupler," in *Proc. Amer. Control Conf.*, San Diego, CA, 1999, pp. 2200–2204.

[13] C. Yang and Y. Sun, "Mixed H_2/H_∞ cruise controller design for high speed train." *Int. J. Control*, vol. 74, no. 9, pp. 905–920, Jun. 2001.

[14] A. Astolfi and L. Menini, "Input/output decoupling problem for high speed trains," in *Proc. Amer. Control Conf.*, Anchorage, AK, 2002, pp. 549–554.

[15] M. Chou, X. Xia, and C. Kayser, "Modelling and model validation of heavy-haul trains equipped with electronically controlled pneumatic brake systems," *Control Eng. Pract.*, vol. 15, no. 4, pp. 501–509, Apr. 2007.

[16] X. Zhuan and X. Xia, "Optimal scheduling and control of heavy trains equipped with electronically controlled pneumatic braking systems," *IEEE Trans. Control Syst. Technol.*, vol. 15, no. 6, pp. 1159–1166, Nov. 2007.

[17] M. Chou and X. Xia, "Optimal cruise control of heavy-haul trains equipped with electronically controlled pneumatic brake systems," *Control Eng. Pract.*, vol. 15, no. 5, pp. 511–519, May 2007.

[18] G. G. Rigatos, "Fuzzy stochastic automata for intelligent vehicle control," *IEEE Tran. Ind. Electron.*, vol. 50, no. 1, pp. 76–79, Feb. 2003.

[19] J. A. Farrell and M. M. Polycarpou, *Adaptive Approximation Based Control: Unifying Neural, Fuzzy and Traditional Adaptive Approximation Approaches*. Hoboken, NJ: Wiley, 2006.

[20] S. S. Ge and C. Wang, "Adaptive neural control of uncertain MIMO nonlinear systems," *IEEE Tran. Neural Netw.*, vol. 15, no. 3, pp. 674–692, May 2004.

[21] M. Chen, S. S. Ge, and B. V. How, "Robust adaptive neural network control for a class of uncertain MIMO nonlinear systems with input nonlinearities," *IEEE Trans. Neural Netw.*, vol. 21, no. 5, pp. 796–812, May 2010.

[22] S. Kumarawwadu and T. T. Lee, "Neuroadaptive combined lateral and longitudinal control of highway vehicles using RBF networks," *IEEE Trans. Intell. Transport. Syst.*, vol. 7, no. 4, pp. 500–512, Dec. 2006.

[23] Y. Boutalis, D. C. Theodoridis, and M. A. Christodoulou, "A new Neuro-FDS definition for indirect adaptive control of unknown nonlinear systems using a method of parameter hopping," *IEEE Trans. Neural Netw.*, vol. 20, no. 4, pp. 609–625, Apr. 2009.

[24] N. J. Cotton and B. M. Wilamowski, "Compensation of nonlinearities using neural networks implemented on inexpensive microcontrollers," *IEEE Trans. Ind. Electron.*, vol. 58, no. 3, pp. 733–740, Mar. 2011.

[25] L. Cheng, Z.-G. Hou, Y. Lin, M. Tan, W. C. Zhang, and F.-X. Wu, "Recurrent neural network for non-smooth convex optimization problems with application to the identification of genetic regulatory networks," *IEEE Trans. Neural Netw.*, vol. 22, no. 5, pp. 714–726, May 2011.

[26] H. Du, S. S. Ge, and J. K. Liu, "Adaptive neural network output feedback control for a class of non-affine non-linear systems with unmodelled dynamics," *IET Control Theory Appl.*, vol. 5, no. 3, pp. 465–477, Feb. 2011.

[27] M. L. Fravolini and G. Campa, "Design of a neural network adaptive controller via a constrained invariant ellipsoids technique," *IEEE Trans. Neural Netw.*, vol. 22, no. 4, pp. 627–638, Apr. 2011.

[28] P. Chen, H. Qin, M. Sun, and X. Fang, "Global adaptive neural network control for a class of uncertain non-linear systems," *IET Control Theory Appl.*, vol. 5, no. 5, pp. 655–662, Apr. 2011.

[29] A. Alessandri, M. Baglietto, G. Battistelli, and M. Gaggero, "Moving-horizon state estimation for nonlinear systems using neural networks," *IEEE Trans. Neural Netw.*, vol. 22, no. 5, pp. 768–780, May 2011.

[30] J.-T. Chan, "Data-based synthesis of a multivariable linear-quadratic regulator," *Automatica*, vol. 32, pp. 403–407, Mar. 1996.

[31] M. Ikeda, Y. Fujisaki, and N. Hayashi, "A model-less algorithm for tracking control based on input–output data," *Nonlin. Anal.*, vol. 47, no. 3, pp. 1953–1960, 2001.

[32] T. S. VanZwieten, G. M. Bower, and S. L. Lacy, "Data-based control of a free-free beam in the presence of uncertainty," in *Proc. Amer. Control Conf.*, 2007, pp. 31–36.

[33] J. Helvoort, B. Jager, and M. Steinbuch, "Data-driven multivariable controller design using ellipsoidal unfalsified control," *Syst. Control Lett.*, vol. 57, no. 9, pp. 759–762, 2008.

[34] H. Y. Yang, S. H. Lee, and M. G. Na, "Monitoring and uncertainty analysis of feedwater flow rate using data-based modeling methods," *IEEE Trans. Nucl. Sci.*, vol. 56, no. 4, pp. 2426–2433, Aug. 2009.

[35] H. Wang, T. Y. Chai, J. L. Ding, and M. Brown, "Data driven fault diagnosis and fault tolerant control: Some advances and possible new directions," *Acta Autom. Sinica*, vol. 35, no. 6, pp. 739–747, Mar. 2009.

[36] Q. Song, Y. D. Song, T. Tang, and B. Ning, "Computationally inexpensive tracking control of high speed trains with traction/braking saturation," *IEEE Trans. Intell. Transport. Syst.*, vol. PP, no. 99, pp. 1–10, Jun. 2011.

[37] A. Boulkroune, M. Tadjine, M. M. Saad, and M. Farza, "Fuzzy adaptive controller for MIMO nonlinear systems with known and unknown control direction," *Fuzzy Sets Syst.*, vol. 161, no. 6, pp. 797–820, Mar. 2010.

[38] W. Cai, X. H. Liao, and Y. D. Song, "Indirect robust adaptive fault-tolerant control of attitude tracking of spacecraft," *J. Guid. Control Dyn.*, vol. 31, no. 5, pp. 1456–1463, Sep.–Oct. 2008.

[39] K. Hornik, M. Stinchcombe, and H. White, "Multilayer feedforward networks are universal approximators," *Neural Netw.*, vol. 2, no. 5, pp. 359–366, Mar. 1989.

[40] R. M. Sanner and J.-J. E. Slotine, "Gaussian networks for direct adaptive control," *IEEE Tans. Neural Netw.*, vol. 3, no. 6, pp. 837–863, Nov. 1992.

[41] A. M. Zou, K. D. Kumar, and Z. G. Hou, "Quaternion-based adaptive output feedback attitude control of spacecraft using Chebyshev neural networks," *IEEE Trans. Neural Netw.*, vol. 21, no. 9, pp. 1457–1471, Sep. 2010.

[42] B. K. Bose, "Neural network applications in power electronics and motor drives – an introduction and perspective," *IEEE Trans. Ind. Electron.*, vol. 54, no. 1, pp. 14–33, Feb. 2007.
[43] N. J. Cotton and B. M. Wilamowski, "Compensation of nonlinearities using neural networks implemented on inexpensive microcontrollers," *IEEE Trans. Ind. Electron.*, vol. 58, no. 3, pp. 733–740, Mar. 2011.
[44] J. Reed and P. A. Ioannou, "Instability analysis and robust adaptive control of manipulators," *IEEE Trans. Robot. Autom.*, vol. 5, no. 3, pp. 381–386, Jun. 1989.

Qi Song is a Ph.D. student with the Center for Intelligent Systems and Renewable Energy, Beijing Jiaotong University, Beijing, China.

Her current research interests include dynamic system modeling, health monitoring, adaptive and fault-tolerant control with application to robotic systems, and high-speed trains.

Yong-Duan Song received the Ph.D. degree from Tennessee Technological University, Cookeville, in 1992.

He was one of the six Langley Distinguished Professors with the National Institute of Aerospace (NIA), Hampton, VA, and the Founding Director of the Cooperative Systems, NIA. He is currently with Beijing Jiaotong University, Beijing, China, and is the Founding Director of the Center for Intelligent Systems and Renewable Energy. His current research interests include intelligent systems, guidance-navigation and controls, bio-inspired adaptive and cooperative systems, and rail traffic controls and safety.

Dr. Song received several competitive research awards from the National Science Foundation, the National Aeronautics and Space Administration, the U.S. Air Force Office, the U.S. Army Research Office, and the U.S. Naval Research Office. He has served as an Associate Editor or Guest Editor for several prestigious scientific journals.